Transverse coupled-bunch instability thresholds in the presence of a harmonic-cavity-flattened rf potential

F. J. Cullinan,[1,*] R. Nagaoka,[1] G. Skripka,[2] and P. F. Tavares[2]
[1]*Synchrotron SOLEIL, Saint Aubin, 91192 Gif-sur-Yvette CEDEX, France*
[2]*MAX IV Laboratory, Lund University, SE-22100 Lund, Sweden*
(Received 19 February 2016; published 16 December 2016)

A small vacuum chamber aperture is a present trend in the design of future synchrotron light sources. This leads to a large resistive-wall impedance that can drive coupled-bunch instabilities. Another trend is the use of passively driven cavities at a harmonic of the main radio frequency to lengthen the electron bunches in order to increase the Touschek lifetime and reduce emittance blowup due to intrabeam scattering. In some cases, the harmonic cavities may be tuned to fulfill the flat potential condition. With this condition met, it has been predicted in simulation that the threshold current for coupled-bunch resistive-wall instabilities is much higher than with no bunch lengthening at all. In this paper, the features of a bunch in the flat potential that would contribute toward this stabilization are identified and discussed. The threshold currents for these instabilities are estimated for the MAX IV 3 GeV storage ring at different values of chromaticity using macroparticle simulations in the time domain and, within the limits of the existing theory, frequency domain calculations. By comparing the results from these two methods and analyzing the spectra of the dominant head-tail modes, the impact of each of the distinguishing features of a bunch in the flat potential can be explained and quantified in terms of the change in threshold current. It is found that, above a certain chromaticity, the threshold current is determined by the radial structure of the zeroth-order head-tail mode. This happens at a lower chromaticity if the bunch length is longer.

DOI: 10.1103/PhysRevAccelBeams.19.124401

I. INTRODUCTION

MAX IV is a synchrotron light source currently under commissioning in Lund, Sweden [1]. It consists of two storage rings and a linac-driven short-pulse facility. The larger storage ring is for a beam of 3 GeV electrons at ultralow emittance. Its main machine parameters are listed in Table I. With the aim of achieving low emittance, the storage ring lattice includes strongly focusing quadrupoles, which are grouped with other types of magnets in combined function magnet blocks. For these quadrupoles to reach high enough gradients, their poles must be close to the beam. For this reason, the radius of the copper beam pipe is very small; its nominal value is 11 mm in both transverse directions [2]. A reduction in the vacuum chamber aperture, a trend for modern light sources, leads to an increase in the resistive-wall impedance, whose transverse dipolar component scales as the inverse aperture cubed [3]. This, in turn, leads to coupled-bunch instabilities that must be damped if a high design beam current, 500 mA in the case of the MAX IV 3 GeV ring, is to be achieved.

The MAX IV 3 GeV ring will employ passively driven cavities at the third harmonic of the main radio frequency (rf) to lengthen the electron bunches. The harmonic cavities do this by altering the rf potential away from the approximately harmonic potential in a single rf system. Above 135 mA, the harmonic cavities of MAX IV may be tuned to the flat potential condition [4]. In this case, the first and second derivatives of the rf potential are zero at the synchronous phase and the bunches are as long as possible without being double-peaked or asymmetric in longitudinal profile. For small synchrotron oscillation amplitudes, the synchrotron tune is no longer approximately the same for all particles but is proportional to their oscillation amplitude. The energy spread in a single bunch is unaffected and the distribution in energy is still close to Gaussian. Conversely, the distribution in longitudinal time offset, although still a natural exponential function, is no longer Gaussian; the exponent is raised to the fourth power instead of the second [5].

The use of harmonic cavities in this way provides many advantages. The lengthening of the bunches means a lower peak bunch current for the same bunch charge and so it increases the Touschek lifetime and reduces emittance dilution due to intrabeam scattering [6]. The synchrotron tune spread introduces Landau damping that has been observed to combat longitudinal instabilities [7–10]. Furthermore, in simulation, harmonic cavities have been shown to increase the threshold current of transverse

*francis.cullinan@synchrotron-soleil.fr

TABLE I. The main parameters of the MAX IV 3 GeV storage ring in the MAX IV facility as used in this paper. The values correspond to the bare machine with no insertion devices.

Parameter	3 GeV ring
Length L_c (m)	528.0
Design beam current (mA)	500
Radio frequency (MHz)	99.931
rf voltage (MV)	1.02
Passive cavity harmonic	3
Horizontal emittance (nm rad)	0.3
Average vertical beta β (m)	6.95
Vertical betatron tune	16.28
Harmonic number h	176
Momentum compacion α_c	3.07×10^{-4}
Natural bunch length σ_τ (ps)	40.0
Lengthened bunch σ_τ (ps)	195
Energy spread σ_δ	7.69×10^{-4}
Energy loss per turn (keV)	363.8
Vertical chamber aperture $2a$ (mm)	22.0
Chamber resistivity ρ (Ωm)	1.7×10^{-8}

instabilities [11]. However, although it may seem intuitive that longer bunches and a spread in synchrotron tune stabilize the beam transversely, the relative importance of each of these factors and any others, is unknown. In this paper, using Laclare's eigenvalue method in the frequency domain and macroparticle simulations in the time domain, the aspects of a harmonic-cavity-lengthened bunch that affect the transverse stability are identified and the contribution of each is quantified. Laclare's eigenvalue method assumes simple harmonic single-particle motion in synchrotron phase space and no synchrotron tune spread. This is approximately true for single-rf systems where the rf potential is close to harmonic but is not true for a system with harmonic cavities tuned to the flat potential condition, where the rf potential is significantly anharmonic. Other frequency domain methods, such as those described in [12,13], are able to include a synchrotron tune spread but only if it is small enough to be treated as a perturbation and so these methods cannot be directly applied to the flat potential condition. The approaches taken in [14,15] do apply directly to a double-rf system but only treat longitudinal instabilities. The time-domain simulations have no such limitations; at the turn-by-turn level, the longitudinal motion of particles in the flat potential condition is faithfully reproduced [16].

Sections I A and I B give brief introductions to, respectively, transverse coupled-bunch instabilities and Laclare's eigenvalue method for calculating their threshold currents. Then, in Sec. II, the results of simulations in the time domain are presented in comparison with frequency domain calculations. These are analyzed in Sec. II A to determine the form of the head-tail modes present. To further investigate the findings, simulations are also performed for an intermediate bunch length of 100 ps, the results of which are presented in Sec. III A. Finally, the effect of adding a broadband resonator to the impedance model is investigated in Sec. III B and overall conclusions that can be drawn are discussed in Sec. IV.

A. Coupled-bunch instabilities

A realistic storage ring has some transverse impedance due to discontinuities in the vacuum chamber and the finite conductivity of the chamber walls. The lowest order transverse impedance is dipolar and is usually normalized by the offset of the exciting particle. Through interaction with the transverse impedance, each particle within a bunch can obtain a betatron phase offset equal to an integer multiple m of its initial azimuthal angle in synchrotron phase space. Such coherent motion is known as an azimuthal head-tail mode and is denoted by its order m, equivalent to the aforementioned integer multiple.

If an ideal beam position monitor (BPM) pick-up with infinite bandwidth and whose output signal is proportional to transverse offset and charge were installed in a storage ring, it would measure the product of the average position offset along the length of a bunch $\langle y \rangle(\tau)$ and the bunch charge distribution in time $g_0(\tau)$. Here, τ is the time offset from the synchronous particle at the center of the bunch. The Fourier transform of this product $\mathcal{F}(\langle y \rangle(\tau) g_0(\tau))$ is referred to as the bunch spectrum σ_m. If the motion of all the particles in the bunch is synchronized ($m = 0$), the bunch spectrum is simply proportional to the Fourier transform of the longitudinal bunch charge distribution $\mathcal{F}(g_0(\tau))$ and is single peaked in most cases. For higher order head-tail modes ($|m| > 0$), the bunch spectrum is double peaked and the two peaks are further apart in frequency the higher the mode order. The amplitude of betatron oscillation may also become dependent on a particle's synchrotron amplitude, leading to some radial structure in synchrotron phase space. In the frequency domain, this gives the head-tail mode the appearance of a higher-order mode.

If the pick-up described above were to measure multiple bunches, uniformly distributed around the ring over many revolutions, a Fourier transform of its output signal could be written as

$$S_m(\omega, \theta) = j^{-m} \pi I \sum_p e^{-jp\theta} \sigma_m(\omega_{mp}) \delta_K(\omega - \omega_{mp} - \Delta\omega_m) \tag{1}$$

where δ_K is the Kronecker delta function, I is the beam current, ω is the angular frequency and θ is the azimuthal angle designating the position in the storage ring where the BPM is installed [17]. It is assumed that only one azimuthal head-tail mode m is present. The spectrum described by Eq. (1) is made up of delta peaks at discrete frequencies given by

$$\omega_{mp} + \Delta\omega_m = (Mp + \mu)\omega_0 + \omega_\beta + m\omega_s + \Delta\omega_m \quad (2)$$

where M is the number of bunches, p is an integer and ω_0, ω_β, and ω_s are the angular revolution frequency, betatron frequency, and synchrotron frequency, respectively. $\Delta\omega_m$ is a coherent frequency shift defined below. With no frequency shift, for the $m = 0$ mode, the peaks are at betatron sidebands to every M^{th} revolution harmonic. For higher order modes ($|m| > 0$), the peaks are at the m^{th} synchrotron sidebands of these betatron lines. Any radial structure does not alter the position of the peaks. A procession of the betatron phase along the train of bunches is known as a coupled-bunch mode and is specified by the integer number of betatron periods μ, also called the coupled-bunch mode number. As with the azimuthal head-tail mode, Eq. (1) assumes that only one coupled-bunch mode is present.

A nonzero chromaticity introduces an additional advance of a particle's betatron phase that is proportional to its longitudinal offset τ. In the frequency domain, this is equivalent to a shift of the bunch spectrum by the chromatic frequency ω_ξ given by

$$\omega_\xi = \frac{\xi\omega_0}{\alpha_c} \quad (3)$$

where ξ is the chromaticity and α_c is the momentum compaction factor of the storage ring.

As a simplification, the whole machine impedance can be modeled as a single dipole impedance at the location of the BPM pick-up. The beam interacts with the storage ring impedance at frequencies ω_{mp} and the strength of the interaction is governed by the bunch spectrum as determined by the particle distribution, the head-tail mode and the chromaticity. The result of the interaction is a complex shift $\Delta\omega_m$ in the coherent betatron frequency of head-tail mode m such that the mode's total coherent frequency Ω_m is given by $\Omega_m = \omega_\beta + m\omega_s + \Delta\omega_m$ where Ω_m and $\Delta\omega_m$ are complex numbers. A positive imaginary part of $\Delta\omega_m$ leads to an exponential growth in the coherent betatron motion. If the growth time is shorter than the transverse radiation damping time, the beam becomes unstable. In cases where the growth time decreases with the beam current, the current at which the growth time is equal to the transverse radiation damping time is known as the threshold current [17].

For reasons of causality, the real part of the machine transverse impedance is an odd function and is positive at positive frequency. In general, it can be said of the real part of the transverse impedance, that where it is positive, it stabilizes the beam and where it is negative, it leads to faster emittance growth. The resistive-wall impedance is large in magnitude at low frequency and so a positive chromatic frequency is generally considered to stabilize the $m = 0$ mode, a mechanism known as head-tail damping. However, this also causes the higher order head-tail modes, which have double-peaked spectra, to become sequentially less stable as their lower peak is moved to a region of larger negative impedance [18].

The features of a bunch in a harmonic-cavity-flattened potential and their influence on transverse coupled-bunch instabilities can now be discussed. First, the lengthening of the bunch corresponds to a narrowing of the bunch spectrum in the frequency domain so that it interacts with a narrower band of the machine impedance. This means that a nonzero chromaticity will be more effective at moving the bunch spectra out of negative frequency and the harmful negative real impedance. Second, the synchrotron tune spread means that the head-tail modes of order $|m| > 0$ are destroyed by decoherence with a mean decay time approximately equal to the inverse of the RMS synchrotron frequency spread. For the MAX IV 3 GeV ring, this is less than a ninth of the radiation damping time so it should naively raise the threshold currents for these modes by about this factor [19]. Third, since the bunch distribution in time in a flat potential is not Gaussian, its spectrum, given by the Fourier transform, will not be single peaked but will have ripples around the central peak that may also interact with the impedance. Finally, the bunch distribution in synchrotron phase space is not radial, i.e., its form in energy is different to its form in time offset so it cannot be expressed as a function of synchrotron amplitude only. This will also have an effect on the bunch spectrum and how it interacts with the impedance.

B. Laclare's eigenvalue method

For small synchrotron oscillation amplitudes in a single-rf potential, it is approximately true that each single particle in a bunch performs simple harmonic motion in synchrotron phase space about the position of the synchronous particle and with the same synchrotron frequency. This is a consequence of the rf potential being approximately harmonic and under this approximation, the complex impedance-driven tune shift for one head-tail mode $\Delta\omega_m$ can be calculated using Laclare's eigenvalue method as outlined in this section. This method can be derived either from an equation of transverse motion of a single particle [20] or as a solution to the linearized Vlasov equation [17]. In both cases, the resulting matrix equation can be written as

$$\Delta\omega_m\sigma_m(\omega_{mq}) = \frac{\beta I}{2T_0E/e}\sum_p jZ_\perp(\omega_{mp})\mathbf{A}^m_{pq}\sigma_m(\omega_{mp}) \quad (4)$$

where T_0 is the revolution time, e is the unit charge, $Z_\perp$ is the transverse impedance, E is the beam energy, I is its current and β is the average transverse beta function. The complex betatron frequency shift $\Delta\omega_m$ for mode m is the eigenvalue with the largest positive imaginary component while the corresponding eigenvector σ_m is the bunch spectrum defined in Sec. I A. Under the approximation

of simple harmonic single-particle motion, the bunch spectrum can also be calculated as

$$\sigma_m(\omega_{mp}) = 2\pi \int_0^\infty J_m[(\omega_{mp} - \omega_\xi)r] g_0(r) Y(r) r dr \quad (5)$$

where J_m is the Bessel function of order m and r is the synchrotron amplitude in units of time, given by

$$r = \sqrt{\tau^2 + \left(\frac{\alpha_c}{\omega_s}\delta\right)^2} \quad (6)$$

where τ is the longitudinal time offset relative to the synchronous particle and δ is the normalized energy deviation. $Y(r)$ is the amplitude of betatron oscillation as a function of the synchrotron amplitude and describes the radial structure of the head-tail mode. $g_0(r)$ is the charge distribution of the bunch in synchrotron amplitude. It is assumed that the different azimuthal head-tail modes do not interact with each other. $\mathbf{A}^m_{pq}$ is a matrix whose elements are given by the function $f_m(\omega_{mp}, \omega_{mq})$ where

$$f_m(x,y) = 2\pi \int_0^\infty J_m[(x - \omega_\xi)r] J_m[(y - \omega_\xi)r] g_0(r) r dr \quad (7)$$

For a radial Gaussian distribution of length σ_τ in time,

$$g_0(r) = \frac{1}{2\pi\sigma_\tau^2} \exp\left(-\frac{r^2}{2\sigma_\tau^2}\right) \quad (8)$$

and the integral in Eq. (7) evaluates to

$$f_m(x,y) = I_m[(x - \omega_\xi)(y - \omega_\xi)\sigma_\tau^2] \times \exp\left[-\frac{(x - \omega_\xi)^2\sigma_\tau^2 + (y - \omega_\xi)^2\sigma_\tau^2}{2}\right] \quad (9)$$

where I_m is the modified Bessel function of order m [17].

As a consequence of the assumed simple harmonic single-particle motion, the bunch charge distribution $g_0(r)$ can only be a function of the synchrotron amplitude r. Formulated in this way, Laclare's eigenvalue method only applies to radial bunch distributions, which have the same form in both energy and time offset. This is not the case in the flat potential condition where the rf potential is anharmonic so that the bunch distribution is close to Gaussian in energy but non-Gaussian in time offset. Laclare's eigenvalue method can therefore not be applied directly to this case. However, it can still be useful for probing the differences between a radial Gaussian bunch and other radial distributions that may have similar longitudinal profiles to a bunch in the flat potential condition. The modes $|m| > 0$ can be ignored because in the flat potential condition, they are destroyed by decoherence and so are not useful to the comparison.

TABLE II. Polynomial distributions inserted into Eq. (7).

Number	Name	(a, b, c)	N	$\hat{r}$
1	Semielliptical	(1, 0, 0)	$\frac{1}{4\pi\sigma_\tau^2}$	$2\sigma_\tau$
2	Flattened	(1, 2, −3)	$\frac{5}{24\pi\sigma_\tau^2}$	$\sqrt{\frac{24}{5}}\sigma_\tau$
3	Double-peaked	(0, 1, −1)	$\frac{3}{2\pi\sigma_\tau^2}$	$2\sigma_\tau$

With $m = 0$, Eq. (7) can be evaluated analytically for radial polynomial distributions with even powers using recursion formulas [21]. The general expression for one such radial distribution is

$$g_0(r) = \begin{cases} N\left(a + b\frac{r^2}{\hat{r}^2} + c\frac{r^4}{\hat{r}^4}\right) & \text{if } 0 \le r < \hat{r} \\ 0 & \text{if } r \ge \hat{r} \end{cases} \quad (10)$$

where a, b, and c are coefficients and N is a normalization constant given by

$$\frac{1}{N} = 2\pi \int_0^{\hat{r}} \left(a + b\frac{r^2}{\hat{r}^2} + c\frac{r^4}{\hat{r}^4}\right) r dr. \quad (11)$$

Three different distributions in synchrotron amplitude have been selected and these are listed in Table II along with their parameters. The profiles for these distributions, that is, their projections onto the temporal axis τ, can be found by integrating Eq. (10) along the energy coordinate between $\pm\sqrt{\hat{r}^2 - \tau^2}$. These are shown in Fig. 1. Distribution 1 is a uniform radial distribution, which appears semielliptical in profile. Distribution 2 has a flattened profile that is most similar to the profile seen in the flat potential condition and

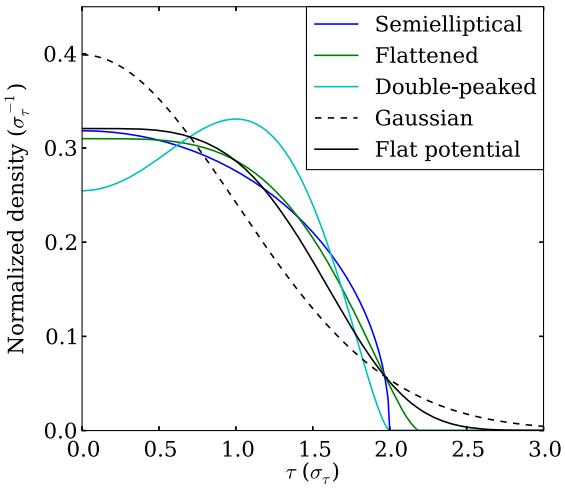

FIG. 1. Bunch profiles for the three non-Gaussian distributions listed in Table II compared to a Gaussian distribution and the distribution expected for the flat potential condition.

the profile of distribution 3 is double-peaked. The three distributions 1, 2, and 3 are therefore referred to as "semielliptical," "flattened," and "double-peaked," respectively. The double-peaked bunch profile may be similar to that of an overlengthened bunch where the harmonic cavity has been tuned beyond the flat potential condition to a regime where there are two minima in the rf potential.

The most common method for calculating the tune shift, besides Laclare's eigenvalue method, is the Sacherer approximation where, instead of an eigenvalue problem which returns both the tune shift and the bunch spectrum, the bunch spectrum is assumed and is then used to calculate the tune shift [22]. The spectra assumed may take the form given by $\sigma_m(\omega_{mp}) = f_m(\omega_{mp}, \hat{\omega})$, where $\hat{\omega}$ is the value of x for which, with zero chromatic frequency, $f_m(x, x)$ is at a maximum, i.e., the frequency at which mode m is expected to be excited most strongly. These are therefore the spectra expected for an excitation by an impedance that is uniform over all frequencies and for most cases, they work for resistive-wall and broadband resonator impedances as well. A head-tail mode excited by a narrowband impedance at frequency ω_r has the form $\sigma_m(\omega_{mp}) = f_m(\omega_{mp}, \omega_r)$ and is known as a shaker mode. Shaker modes with the same azimuthal index m excited at different resonant frequencies differ in their radial structure [20,23].

When solving both Laclare's eigenvalue method and the Sacherer approximation, the summation over frequency (index p in Eq. (4) can be truncated since at high frequency, the magnitude of the bunch spectrum tends to zero for all head-tail modes. Furthermore, this happens at lower frequency for the most dominant low-order head-tail modes. Laclare's method is computationally more expensive than the Sacherer approximation because it is a matrix eigenvalue problem rather than a formula with a couple of summations. However, it has the advantage that the bunch spectrum is not fixed and so it is applicable to cases where the spectrum is significantly distorted because of the radial structure of the head-tail mode.

II. SIMULATIONS

In order to separate the four possible contributions of a harmonic cavity to the beam stability, which are described in Sec. I A, macroparticle simulations of the MAX IV 3 GeV bare ring with all rf buckets filled were run for three different cases: 1. Effects of the harmonic cavities not included and otherwise nominal parameters so that the RMS bunch length is 40 ps. 2. Bunch length increased to the nominal lengthened value of 195 ps by ignoring the energy loss due to synchrotron radiation (stationary beam) and by lowering the rf voltage to 0.04 MV. By lengthening in this way without increasing the momentum compaction factor (affecting the chromatic frequency) or the energy spread, the bunch maintains its radial Gaussian distribution and does not acquire a significant synchrotron tune spread. 3. All the nominal machine parameters and an active harmonic cavity providing the flat potential condition for all bunches. The bunch length is therefore also 195 ps but in addition, the effects of the synchrotron tune spread and modified beam distribution are present.[1] The results of the simulations were compared with calculations performed in the frequency domain. For the short bunch case (1) and the lengthened Gaussian bunch case (2), the frequency domain calculations assume a Gaussian distribution. For the flat potential case (3), the $|m| > 0$ modes are ignored since they are expected to be destroyed by the decoherence due to the synchrotron tune spread and the frequency domain calculations are performed for the bunch distributions in Table II. As previously stated, the nonradial bunch distribution in synchrotron phase space and single-particle motion that is not simple harmonic are not accounted for by the frequency domain calculations. All the simulations were performed for the vertical plane and with the resistive-wall impedance only, which is given by

$$Z_\perp(\omega) = \frac{\mu_0 L_c c}{a^3}\sqrt{\frac{\rho}{2\pi\mu_0|\omega|}}\left(\frac{\omega}{|\omega|} + j\right) \tag{12}$$

where μ_0 is the permeability of free space, c is the speed of light and the other symbols are defined in Table I. Without insertion devices, the horizontal plane is not expected to be very different besides the radiation damping time being lower due to the dispersion.

The macroparticle tracking code used for the time domain simulations was MBTRACK [16], which is able to treat both the long and short-range effects of the resistive-wall impedance for multiple bunches and applies the effects of the impedance once per turn. For the short-range wakefield, the macroparticles are binned according to their longitudinal position within the bunch and their transverse position offsets are summed to obtain the dipole moment of each bin. A discrete convolution of this with the wake function is then performed to calculate the kicks that should be applied to the macroparticles in each bin, thus taking the finite bunch length into account. For the long-range wakefield, the dipole moments of each bunch are stored over a number of turns and the contributions of each are summed to calculate the kick to apply to all the macroparticles in each bunch. The effect of the finite bunch length on the long-range wake is neglected because the narrowband component of the resistive-wall impedance is centered at zero frequency and so it is the dipolar bunch motion that is important. The code was run with no radiation damping or quantum excitation; instead, the longitudinal bunch distribution was imposed from the beginning. MBTRACK calculates the Courant-Snyder invariant of each individual macroparticle as

[1] An active harmonic cavity was used to minimize the simulation time. It has been shown using macroparticle tracking [24] and numerical calculations [4] that the same flat potential condition can be achieved using passive cavities as long as their shunt impedance is sufficient for the beam current.

$$\epsilon_y(y, y') = \gamma y^2 + 2\alpha y y' + \beta y'^2 \tag{13}$$

where γ, α, and β are the Twiss parameters ($\alpha = 0$, $\gamma = 1/\beta$ in these simulations) and y and y' are the macroparticle's position offset and normalized transverse momentum, respectively. The average over all the particles $\langle \epsilon_y \rangle$ is then taken as the emittance of the bunch. This was calculated between every 5 to 25 thousand turns, depending on the simulation length, and the growth rate was determined using a linear fit to the natural logarithm of the square root of the last five values, the emittance being proportional to the square of the betatron amplitude. Assuming a growth rate directly proportional to the beam current [as in Eq. (4)], with constant of proportionality k_I, the threshold current for the instability I_{th} could be calculated as

$$I_{\text{th}} = \frac{1}{k_I \tau_y} \tag{14}$$

where τ_y is the radiation damping time in the vertical plane. 10,000 macroparticles per bunch were used in the simulations and a dipole-moment history length of 300 turns was used to calculate the kicks from the long-range resistive-wall wakefield. The number of turns tracked was dependent on how quickly the instability developed so that the growth rate could be measured. The shortest simulations run were of 200,000 turns while the longest were of several million. All the simulations were performed with a beam current of 100 mA in order to keep the perturbation small and to avoid any interaction between the different head-tail modes.

The code used for the frequency domain calculations was RWMBI [25]. It solves Eq. (4) for the eigenvalues and was extended to include the distributions listed in Table II in addition to the Gaussian distribution it assumes by default. The calculation was performed for all 176 coupled-bunch modes in the MAX IV 3 GeV ring and for head-tail modes $m < 3$, which were found to limit the threshold current in the chromaticity ranges considered. Each data point in the frequency domain results shown in the figures in this section represents the threshold current of the coupled-bunch mode with the highest growth rate. As expected from the resistive-wall impedance, it is the coupled-bunch mode of lowest negative frequency (-1) that is almost always the least stable. The only exceptions were with the $|m| > 0$ modes at zero chromaticity and the $m = 0$ mode in the short bunch case in the ranges of chromaticity where its threshold current was above 500 mA.

Figure 2 shows the results for the first case of the short bunch in the single rf system. The time domain simulation always returns the minimum threshold current seen in the frequency domain calculations and there is excellent agreement between the two. The threshold current behaves as expected, with the $m = 0$ mode being stabilized then the higher-order modes sequentially becoming more unstable as the chromaticity is increased. This behavior is also seen when the Sacherer approximation is applied and follows the general explanation of the different head-tail modes being sequentially stabilized as their peaks are moved away from small negative frequencies where the real part of the impedance is large and negative. A comparison between Laclare's eigenvalue method and the Sacherer approximation, both evaluated using RWMBI, is shown in Fig. 3. Since the main rf at MAX IV (99.931 MHz) is low compared to other storage rings, the bunch length is already sufficiently long that for high chromaticities, the two methods diverge considerably. This is because there is sufficient distortion of the head-tail modes that the Sacherer approximation, which

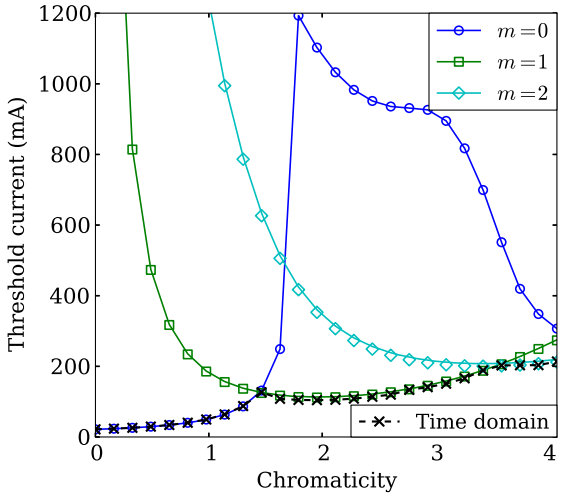

FIG. 2. Threshold current for the coupled-bunch resistive-wall instability for the case with a short bunch in a single rf system. Results of macroparticle simulations in the time domain (dashed line) are compared with those obtained using a frequency domain computation (solid lines).

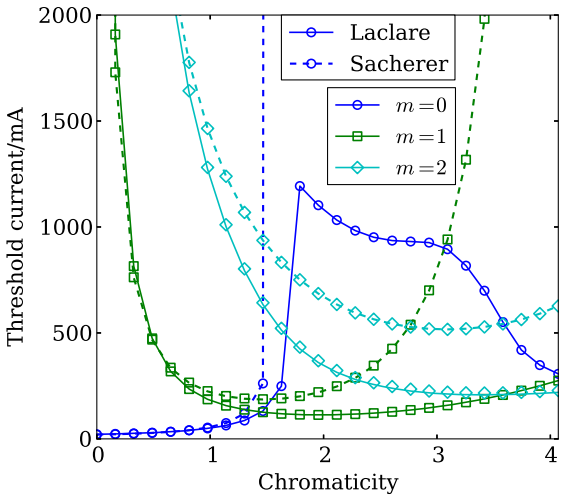

FIG. 3. Comparison of the Laclare eigenvalue method with the Sacherer approximation when both are applied to the case of the short bunch in a single RF system.

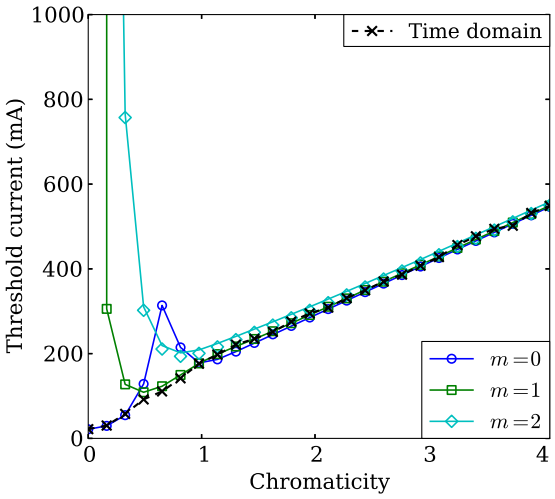

FIG. 4. Threshold current for the coupled-bunch resistive-wall instability for the case with a stationary, lengthened Gaussian bunch. Results of macroparticle simulations in the time domain (dashed line) are compared with those obtained using a frequency domain computation (solid lines).

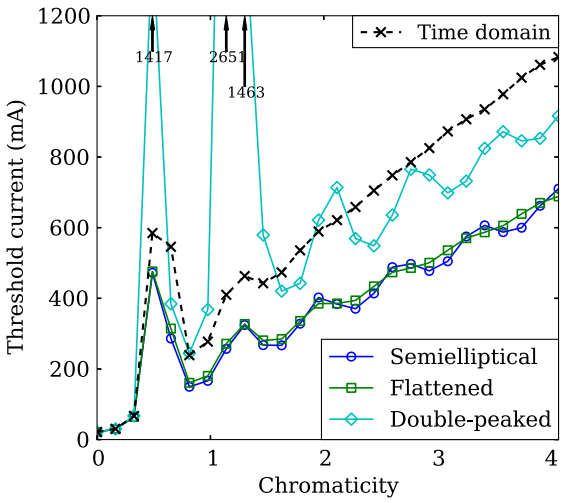

FIG. 5. Threshold current for the coupled-bunch resistive-wall instability for the case with a harmonic cavity flat potential. Results of macroparticle simulations (dashed line) in the time domain are compared with those obtained using a frequency domain computation of the $m = 0$ head-tail mode for three non-Gaussian distributions (solid lines).

assumes one head-tail mode spectrum for each mode at all chromaticities, fails to follow. The difference is most extreme for the $m = 0$ mode above a chromaticity of 1.8. The Sacherer approximation predicts an indefinite stabilization of this mode while Laclare's eigenvalue method predicts that for chromaticities above 1.8, the mode is destabilized as the chromaticity is increased further.

Figure 4 shows the results for the lengthened Gaussian bunch. As anticipated, the $m = 0$ mode is stabilized at a lower chromaticity than with the shorter bunch. However, it is also destabilized at lower chromaticity. Above a chromaticity of 1, all three head-tail modes appear to have very similar threshold currents that increase linearly with chromaticity. Once again, this would not be seen with the Sacherer approximation, where all modes would limit the threshold current sequentially, as in the case of the short bunch. It is clear that for this bunch length, the dynamics is in a regime well beyond the reach of the Sacherer approximation. It is, in fact, only between a chromaticity of 0.45 and 1 that a head-tail mode of higher than zeroth order ($m = 1$) limits the threshold current. Therefore, if the $m = 1$ mode were removed without changing the bunch distribution, by introducing a large spread in the synchrotron tune, for example, it would only affect the threshold current in this range of chromaticities.

The results for the flat potential condition are shown in Fig. 5. The frequency domain results that have been included are the beam distributions for the $m = 0$ mode listed in Table II. With the Gaussian distribution, a smooth trend in the threshold current can be seen across the range of coupled-bunch modes. However, with the alternative distributions, a few of the 176 coupled-bunch modes showed anomalously low threshold currents, probably due to some numerical error. For these cases, the eigenvectors extracted from the calculation were also very different from the bunch spectra expected, i.e., those described in Sec. I A. These anomalous results were therefore filtered out. All modes $|m| > 0$ should be destroyed by decoherence because of the spread in the synchrotron tune and so these were neglected. The agreement between the results from the time domain and those from the frequency domain is not as good as in the other two cases because Laclare's eigenvalue method is unable to treat the nonradial bunch distribution seen with the flat potential condition. However, the results from the two methods do share some common features, in particular, the large peak at a chromaticity of 0.5. This suggests that, unlike in the lengthened Gaussian case, the $m = 1$ mode does not limit the threshold current in this region. As the chromaticity is increased further, in the time domain results, a slight peak is visible at $\xi = 1.3$ and then the threshold current increases linearly as in the lengthened Gaussian case. The frequency domain results replicate this peak and show more peaks at higher chromaticities. This behavior can be understood by looking at the Fourier transform of the bunch profiles in each case, shown in Fig. 6. Unlike the Gaussian distribution, which is also Gaussian in the frequency domain, the Fourier transforms of the non-Gaussian distributions do not simply have a single peak at zero frequency but also ripples at higher frequencies that get smaller as the frequency is increased. For the distributions used in the frequency domain calculations, these ripples are much larger than those of the flat potential distribution. In the time domain, these ripples correspond to the tails of the bunch profile. They are larger

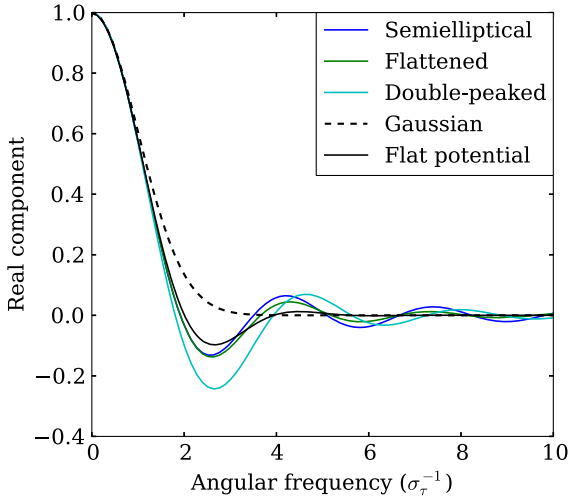

FIG. 6. Fourier transform of the three non-Gaussian distributions listed in Table II compared to a Gaussian distribution and the distribution expected for the flat potential condition.

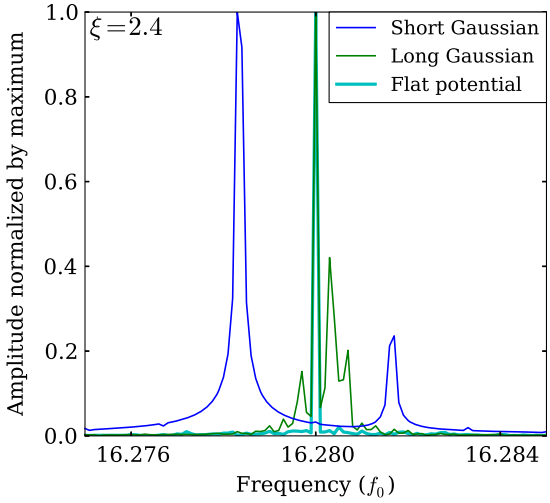

FIG. 7. Fourier transform of the beam signal around the first betatron tune line from tracking of beam distributions produced in time domain simulations of coupled-bunch instabilities at a chromaticity of 2.4. The frequency axis is given in terms of the revolution frequency f_0.

for the three approximate distributions because these distributions all have discontinuities where the charge reaches zero whereas the bunch distribution in the flat potential approaches zero asymptotically with time offset. It is the ripples that cause the peaks in the threshold currents above a chromaticity of 1, as explained further in Sec. II A.

The frequency domain and time domain results displayed in Fig. 5 differ significantly in the absolute values for the threshold current. The semielliptical and flattened bunch profiles predict threshold currents that are only slightly above those for the lengthened Gaussian case whereas the time domain results show threshold currents that are, at high chromaticity, more than 50% above these thresholds. It is concluded that it is the nonradial distribution in synchrotron phase space, which is not accounted for in the frequency domain calculations, that explains this difference. The difference between the semielliptical and flattened profiles suggests that the form of the bunch profile does not affect the threshold currents to the same extent. The double-peaked distribution gives threshold currents that are higher but, at large values of chromaticity, still not as high as the time domain results and the peaks seen are a lot bigger than in the time domain.

A. Modal analysis

In order to further interpret the results, the form of the bunch spectra in each region of the chromaticity scan was investigated. This can be done in both the frequency domain and the time domain. In the frequency domain, they are simply given by the eigenvectors σ_m. In the time domain, the macroparticle distribution of a single bunch is saved at the end of the simulation of the instability. This is then tracked around the ring for 10,000 turns with no impedance effects. The product of the position offset $\langle y \rangle(\tau)$ and the longitudinal bunch distribution $g_0(\tau)$, as would be measured by the infinite bandwidth BPM pick-up described in Sec. I A, can then be saved every turn. In practice, this is done using the binning system of MBTRACK, which bins the particles according to their longitudinal time offset τ and then sums their offsets to arrive at this product. The beam signal in the frequency domain can then be calculated by taking a discrete Fourier transform, accounting for the many zeros between turns:

$$S(\omega) = \sum_{l=0}^{L-1} \left(\sum_{k=0}^{K-1} N_{lk} \langle y \rangle_{lk} e^{-j\omega \Delta t_s (k + l\frac{\omega_0 \Delta t_s}{2\pi})} \Delta t_s \right) \tag{15}$$

where L is the number of turns tracked, K is the number of bins, Δt_s is the bin width in time, and N_{lk} and $\langle y \rangle_{lk}$ are the number of particles in bin k at turn l and their average transverse offset, respectively. From Eq. (1), the bunch spectrum $\sigma_m(\omega_{mp})$ is proportional to $S(\omega_{mp})$. The form of the bunch spectrum can therefore be obtained by solving Eq. (15) at the discrete frequencies ω_{mp}. For this to be strictly true, the values for ω_0, ω_β, and ω_s used in the simulation must all be exact multiples of $2\pi/\Delta t_s$ [20].

Figure 7 shows the spectra of the beam signals from the time domain simulations around the first betatron tune line for a chromaticity of 2.4. For the short Gaussian bunch, peaks can clearly be seen at the upper and lower synchrotron sidebands suggesting the presence of the ± 1 head-tail modes.[2] The peak at the betatron tune ($m = 0$) is much

[2]Either the positive or negative head-tail mode (usually the negative) will be slightly more unstable but the difference between them in the frequency domain results was found to be negligible.

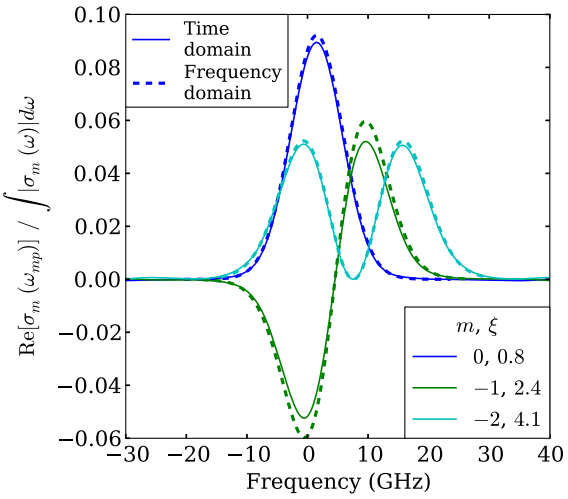

FIG. 8. Transverse bunch spectra for the short bunch case for the dominant mode at three different chromaticities. Time domain and frequency domain results are compared.

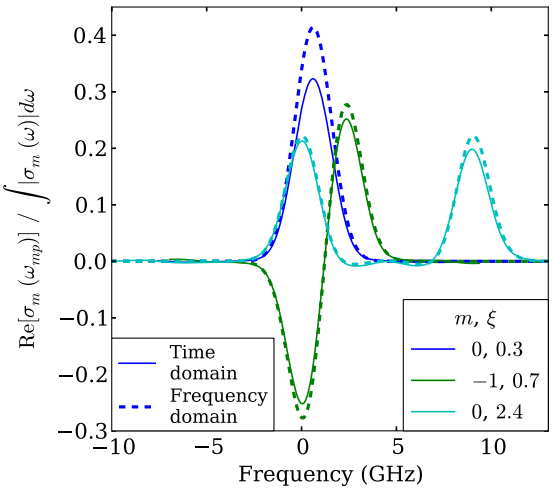

FIG. 9. Transverse bunch spectra for the lengthened Gaussian bunch case for the dominant mode at three different chromaticities. Time domain and frequency domain results are compared.

smaller in comparison. For the lengthened bunch case, many modes appear to be present but the dominant one is $m = 0$. The other modes are also closer to the central peak because of the lower synchrotron tune. Finally, for the flat potential condition, there is only a single peak at the fractional betatron tune. This confirms that the decoherence of the higher than zeroth order modes is strong.

At low chromaticity, for all three cases, the head-tail modes have the form expected and that would be used for the Sacherer approximation, that is a single peaked Fourier transform of the longitudinal bunch charge distribution for $m = 0$ and a double peaked spectrum for the other head-tail modes. Figure 8 shows the bunch spectra of three different head-tail modes for the short bunch case, each at a chromaticity where the mode shown limits the threshold current. The spectra of the three different modes have the expected form.

For the lengthened Gaussian bunch, for three different chromaticities in regions of interest, the spectra of the threshold-current-defining head-tail modes are shown in Fig. 9. At low chromaticity, the bunch spectrum of the $m = 0$ mode is single peaked. As the chromaticity is increased, this peak is shifted to positive chromaticity, leading to some stabilization. At this point, the $m = -1$ head-tail mode, which has a spectrum similar to the spectrum of the same mode in the short bunch, begins to define the threshold current. Then, at the peak in the threshold current of the $m = 0$ mode, its spectrum becomes double peaked. It is this transition in the $m = 0$ spectrum that causes its threshold current to not increase indefinitely as the chromaticity is increased but to begin to decrease and then limit the overall threshold current at high chromaticity.

At one point in the regime where the threshold current is increasing linearly with chromaticity, the spectra of three different modes are shown in Fig. 10. It can be seen here that the spectra of all three head-tail modes are double peaked and the separation between the peaks is the same, twice the chromatic frequency. This means that the lower peak is nearly always centered at zero frequency, where the resistive-wall impedance is largest. As the chromaticity is increased, the separation between the two peaks increases and their height decreases so that the overall effect is the linear increase in the threshold current. From inspection of the distribution of particle offsets in synchrotron phase space at the end of the instability simulation, shown in Fig. 11, it is clear that there is some radial structure to the head-tail modes that gives the double-peaked spectra in the frequency domain. It is in the radial structure that the mode spectra returned by Laclare's eigenvalue method differ from those assumed in the Sacherer approximation, in which, the

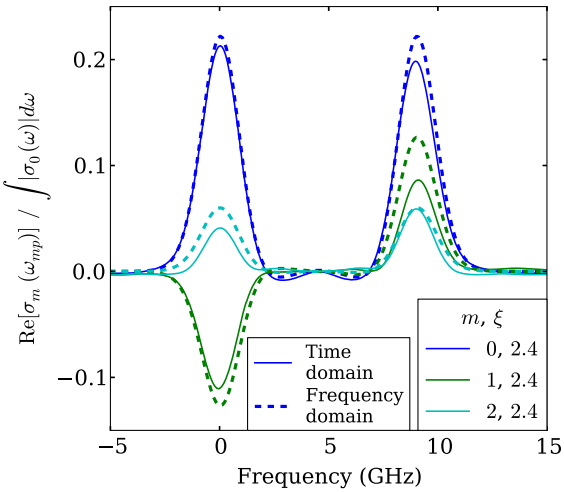

FIG. 10. Transverse bunch spectra for the lengthened Gaussian bunch case for the dominant mode at three different chromaticities.

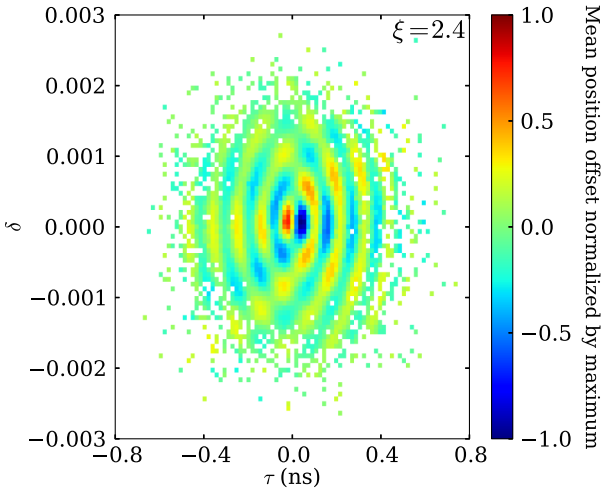

FIG. 11. Scatter plot of populated bins in synchrotron phase space for the lengthened Gaussian bunch at the end of a macroparticle simulation of a coupled-bunch instability at a chromaticity of 2.4. The color of each point represents the mean offset of particles within that bin.

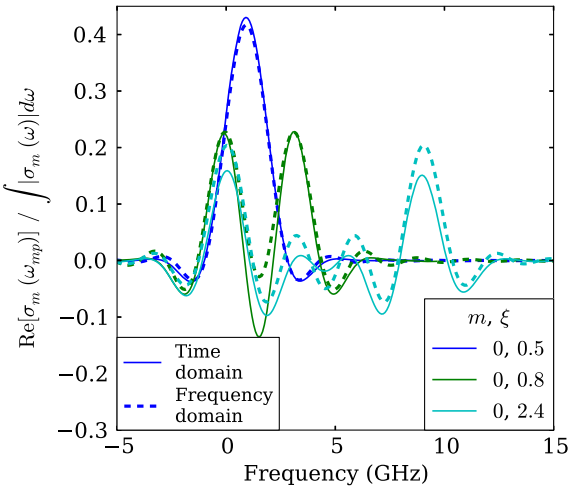

FIG. 12. Transverse bunch spectra in the flat potential condition for the $m = 0$ mode at three different chromaticities. The frequency domain spectra are for the flattened bunch profile.

radial and azimuthal geometry of the mode is fixed and only the phase offset due to the chromaticity changes. Laclare's eigenvalue method covers every possible radial structure for each azimuthal mode number. The radial structure seen is the one that is the least stable against the impedance and when this differs considerably from what is most commonly expected for that azimuthal mode number, the predictions obtained using the two methods differ greatly. This happens at lower chromaticity for longer bunch lengths since the commonly expected bunch spectra are narrower and so, for moderate chromaticities, do not cover the frequencies where the impedance is large, around zero frequency in the case of the resistive-wall impedance.

The results for the flat potential condition are shown in Fig. 12 along with frequency domain calculations using the flattened bunch profile. As the chromaticity is increased from zero, the spectrum of the $m = 0$ mode shows similar behavior to that seen in the lengthened Gaussian case. The $m = 1$ mode, on the other hand, does not limit the threshold current at any point since all the $|m| > 0$ modes are destroyed by the decoherence. The peak in the threshold current of the $m = 0$ mode when its spectrum becomes double peaked is therefore visible, even in the results of the time domain simulations. In the high chromaticity regime, the bunch spectrum continues to behave similarly to the lengthened Gaussian case. However, because the Fourier transform of the bunch profile has ripples around the main peak, the two peaks in the bunch spectrum have some oscillatory structure between them. As the chromaticity is increased, not only do the two main peaks get smaller but the number of oscillations between them increases. It is the addition of these oscillations that causes the threshold current to peak at certain chromaticities above that of the first peak. The smaller the ripples in the frequency domain profile, the smaller the peaks in the threshold current. As with the lengthened Gaussian bunch case, there is a visible radial component to the coherent motion within the bunch, see Fig. 13.

The form of the bunch spectra for both cases with lengthened bunches is similar to shaker modes being excited by a narrowband impedance at zero frequency. Figure 14 shows a comparison between the eigenmodes from the frequency domain computation and these shaker modes excited at zero frequency at a chromaticity of 2.4. This shows that the beam is behaving as would be expected with a strong excitation at zero frequency, as is the case

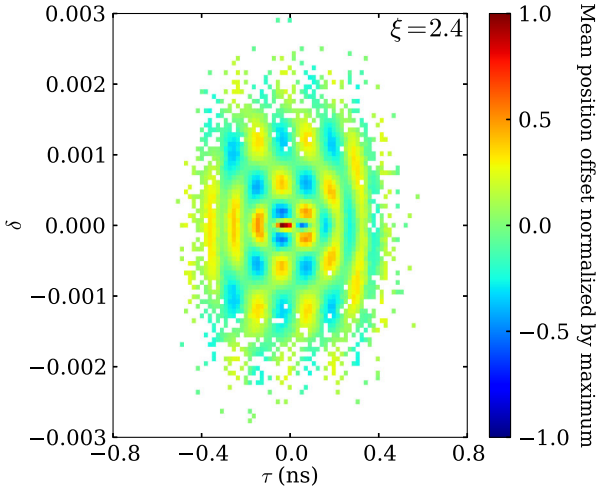

FIG. 13. Scatter plot of populated bins in synchrotron phase space for the flat potential condition at the end of a macroparticle simulation of a coupled-bunch instability at a chromaticity of 2.4. The color of each point represents the mean offset of particles within that bin.

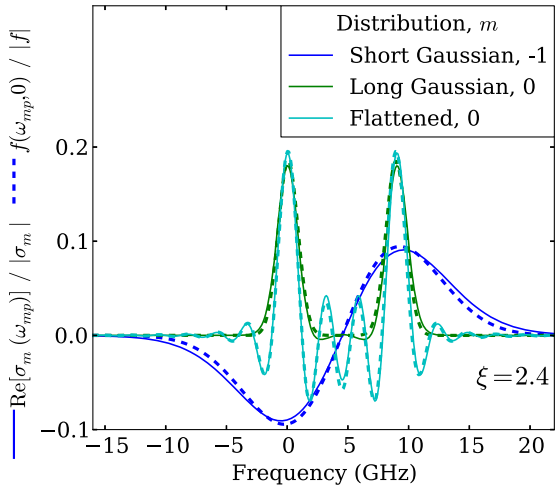

FIG. 14. Comparison of the transverse bunch spectra σ_m for three different beam types at a chromaticity of 2.4 with their corresponding shaker modes excited at zero frequency $f(\omega_{mp}, 0)$.

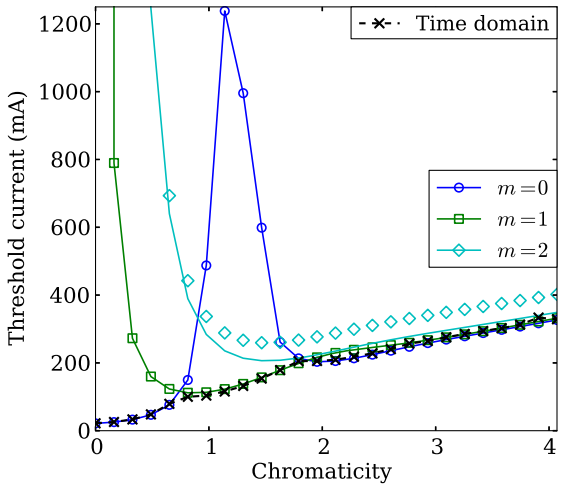

FIG. 15. Threshold current for the coupled-bunch resistive-wall instability for the case with a Gaussian bunch at an intermediate length of 100 ps. Results of macroparticle simulations in the time domain (dashed line) are compared with those obtained using a frequency domain computation (solid lines).

with the resistive-wall impedance. This explains why the separation between the two peaks in the spectra of the lengthened bunches is twice the chromatic frequency. The eigenmodes resemble the shaker modes less at some chromaticities than at others and even small differences can cause a large change in the threshold current when they are at frequencies where the impedance is large. Interpreting the problem only as a narrowband excitation at zero frequency, by inserting these shaker modes into the Sacherer approximation for example, would therefore lead to errors.

III. OTHER CASES

In order to further understand the results in Sec. II, similar investigations were performed for an intermediate bunch length of 100 ps. The study was then extended to briefly look into the effects of a broadband resonator impedance.

A. Intermediate bunch length

A Gaussian bunch of an intermediate length of 100 ps was generated by lowering the rf voltage to 0.15 MV with the stationary beam. The same bunch length was also achieved with the flat potential condition by introducing an active harmonic cavity at the 11th harmonic of the main rf. Figure 15 shows the frequency and time domain results for this intermediate length case with the Gaussian bunch. As the chromaticity is increased from zero, the peak seen in the threshold current of the $m = 0$ mode when its spectrum becomes double peaked, is higher than in the case of the full-length Gaussian bunch (see Fig. 4). Then, as the chromaticity is increased further, the $m = 1$ mode is also slightly stabilized and destabilized again. Apart from these details, it becomes clear that the result of the change in bunch length is mostly a linear scaling along the horizontal axis. The details are caused by the fact that the shorter the bunch length, the wider the bunch spectrum and so the greater the number of frequency lines in Eq. (2) that become important in the interaction of the beam with the impedance.

The threshold curve for the flat potential case with the medium length bunch is shown in comparison with the frequency domain results in Fig. 16. As with the full-length bunch in the flat potential, for which the equivalent plot is

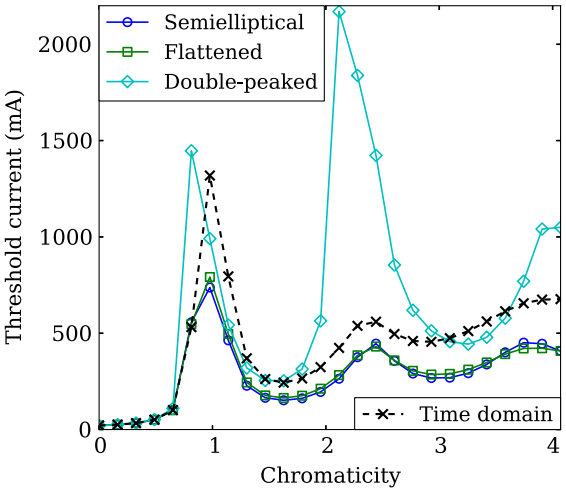

FIG. 16. Threshold current for the coupled-bunch resistive-wall instability for the case with a potential flattened with a harmonic cavity at the 11th harmonic of the main rf. Results of macroparticle simulations in the time domain (dashed line) are compared with those obtained using a frequency domain computation (solid line).

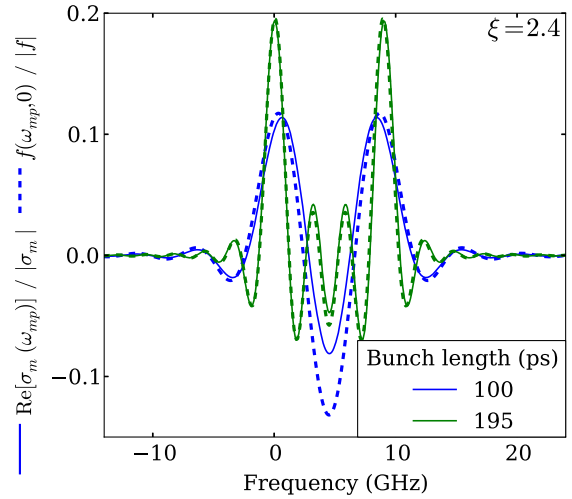

FIG. 17. Comparison of the transverse bunch spectra σ_m for the flat potential condition, a chromaticity of 2.4 and two different bunch lengths with the corresponding shaker modes excited at zero frequency $f(\omega_{mp}, 0)$.

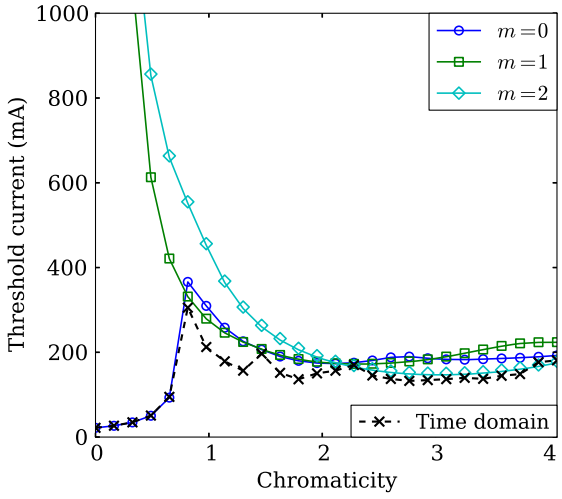

FIG. 18. Threshold current for the coupled-bunch resistive-wall instability in the 3 GeV ring with a BBR included for the case with a short bunch in a single rf system. Results of macroparticle simulations in the time domain (dashed line) are compared with those obtained using a frequency domain computation (solid lines).

shown in Fig. 5, there are peaks in the threshold current but they are found to be more pronounced. Ultimately, this means that at certain chromaticities, the intermediate length bunch is predicted to be more stable than the full-length bunch in the flat potential. Again, the inverse scaling with bunch length is clear across the full range of chromaticity.

Figure 17 shows the bunch spectra for the flattened bunch profile, calculated in the frequency domain, in comparison with the corresponding shaker modes at a chromaticity of 2.4. At this chromaticity, there is a peak in the threshold current for the intermediate bunch length. As with the peaks seen with the fully-lengthened case, it occurs as oscillations appear between the two main peaks in the bunch spectrum. It can be seen in the figure that, for the intermediate bunch length, the increase in chromaticity has moved the lower peak in the bunch spectrum to a slightly positive frequency and to a higher frequency than the peak in the shaker mode. This leads to some stabilization and the peak seen in the threshold current. As the chromaticity is increased above 2.4, another oscillation appears between the main peaks and their separation in frequency increases. This moves the lower peak back toward negative frequency and causes some destabilization. This process occurs with the fully lengthened bunch as well but to a lesser extent so that it is less easy to see in the bunch spectra and the resulting peak in the threshold current is smaller. The reason for the difference in the size of the effect is the greater number of frequency lines covered by the wider bunch spectrum of the shorter, intermediate-length bunch.

B. Broadband resonator

A broadband resonator (BBR) at 6.38 GHz and with a shunt impedance of 0.065 $\mathrm{M\Omega m^{-1}}$ and a quality factor of unity was introduced into the simulations. This is one of the strongest BBRs in the impedance model of the MAX IV 3 GeV ring [11]. MBTRACK has not yet been extended to treat the long-range effects of resonant transverse wakefields but since the quality factor is so low, these should be negligible.

With the BBR, the results for the short bunch are shown in Fig. 18. The time domain simulations predict a couple of dips in the threshold current between chromaticities of 1 and 2 that do not appear in the frequency domain results but the overall agreement between the two is still good. The effect of the BBR is to stabilize the $m = 0$ and $m = 1$ head-tail modes so that the threshold current is higher up to a chromaticity of about 3. Above this chromaticity, all the modes are destabilized leading to a threshold current that is lower than without the BBR. When the Gaussian bunch is lengthened, as is the case in Fig. 19, the BBR also stabilizes the $m = 2$ mode because the lengthening brings this mode below the frequency of the BBR. The peak in the threshold current for the $m = 0$ mode at a chromaticity of around 0.5 is a lot higher than in the case without the BBR and, similar to with the intermediate bunch length, the $m = 1$ mode is also stabilized and then destabilized as the chromaticity is increased. The BBR is responsible for an additional peak in the threshold currents of all head-tail modes at a chromaticity of around 1.5. Above this, all the modes are destabilized and their threshold currents are the same. Above a chromaticity of 2.5, their thresholds all increase linearly with chromaticity but with a lower gradient than in the case with no BBR.

With the flat potential condition, the behavior is as shown in Fig. 20 where again, only the $m = 0$ mode is

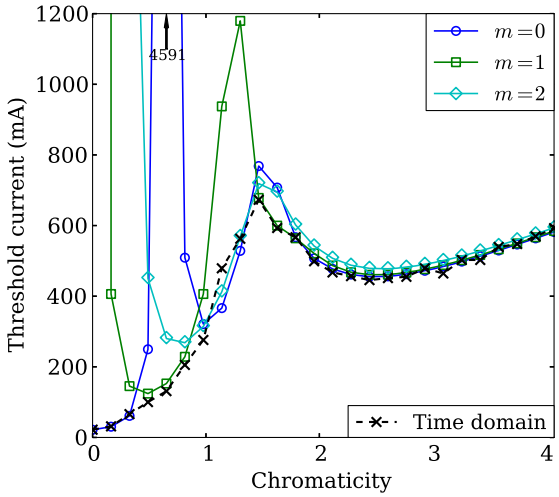

FIG. 19. Threshold current for the coupled-bunch resistive-wall instability in the 3 GeV ring with a BBR included for the case with a lengthened Gaussian bunch. Results of macroparticle simulations in the time domain (dashed line) are compared with those obtained using a frequency domain computation (solid lines).

considered. Once again, the peak around a chromaticity of 0.5 is much larger than in the case without the BBR. In fact, for the time domain simulation, one threshold current could not be calculated because the instability was not seen after six million turns of tracking. This may mean that the $m = 0$ mode is actually being damped at this chromaticity. The peaks at higher chromaticity are also larger and appear in both the frequency and time domain. Since the bunch length is the same as for the lengthened Gaussian case, it is expected that a peak caused directly by the BBR would be

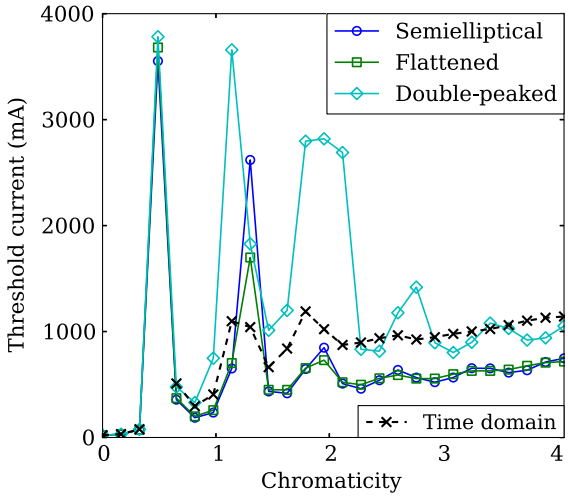

FIG. 20. Threshold current for the coupled-bunch resistive-wall instability in the 3 GeV ring with a BBR included for the case with a harmonic cavity flat potential. Results of macroparticle simulations in the time domain are compared with those obtained using a frequency domain computation of the $m = 0$ head-tail mode for three non-Gaussian distributions.

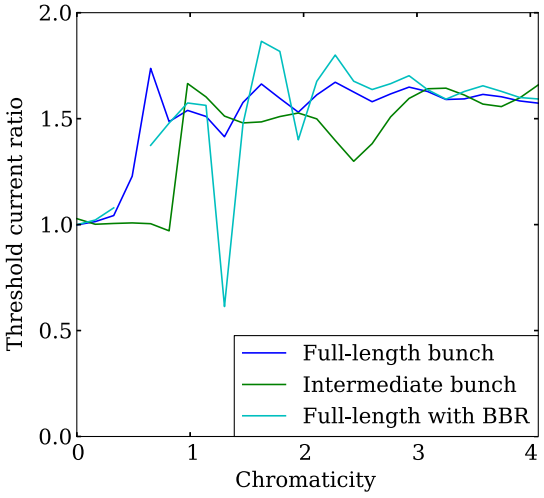

FIG. 21. Ratio of threshold currents predicted by time domain simulations of the flattened potential to those predicted by frequency domain calculations for a flattened bunch distribution with the same bunch length.

in the same place. However, the periodicity caused by the oscillations between the main peaks in the bunch spectra appears to dominate. The effect that the BBR has here is that the peaks that are above a chromaticity of 1.5 (where the peak appears in the lengthened Gaussian bunch case) are shifted to a lower chromaticity. Once again, the overall linear increase in threshold current above a certain chromaticity, in this case 2, is present but with a lower gradient than in the case with no BBR. Overall, this leads to a lower threshold current above a chromaticity of 3.

The ratio between the threshold currents predicted by the time domain simulations of the flat potential condition and the frequency domain calculations based on the flattened bunch profile is shown for both bunch lengths simulated and with and without the BBR in Fig. 21. It can be seen that, at high chromaticity especially, this ratio is almost constant, around 1.6. At low chromaticity, this value is reached from below at a point that coincides with the first peak in the threshold current. This ratio was found to be independent of the rf harmonic chosen for the operation of the harmonic cavities and for another machine simulated. It suggests that, at high chromaticity, the influence of the nonradial distribution in synchrotron phase space is simply a constant factor, by which the right-hand side of Eq. (4) could be multiplied.

IV. CONCLUSION

In a storage ring, a flattened longitudinal potential, as can be obtained using harmonic cavities, can increase the threshold current of transverse coupled-bunch instabilities. There are four features of a beam in a flat potential that contribute to this: the lengthened bunch, the synchrotron tune spread and two concerning the bunch's synchrotron-phase-space distribution: first, that it is non-Gaussian and

second, that it is not radial. The contribution of each of these four features to the instability threshold current has been studied using a model of the resistive wall impedance and its interaction with bunches uniformly distributed around the MAX IV 3 GeV ring.

The effect of the increase in bunch length has been investigated by comparing simulations of a short bunch in a single rf system and a bunch lengthened in such a way that no significant synchrotron tune spread is introduced. The longer bunch means that the lowest order single bunch head-tail modes are stabilized at a lower chromaticity. However, as the chromaticity is increased further, a regime is reached where the spectra of all these modes become double peaked due to their radial structure and are destabilized. One of the two peaks is centered close to zero frequency as this is where the resistive-wall impedance is strongest while the other is at around twice the chromatic frequency. If a resonant impedance, like a dipolar higher order mode in a rf cavity, was driving the instability, it is expected that one peak would instead be centered at the resonant frequency of this mode. The radial structure to the head-tail mode changes to the extent that the Sacherer approximation and the physical interpretation attached completely break down. All head-tail modes have the same threshold current that increases linearly with chromaticity.

The synchrotron tune spread means that modes with index $|m| > 0$ are destroyed by decoherence, as quickly as in a ninth of the radiation damping time in the case of the MAX IV 3 GeV ring [19]. This means that the peak in the threshold current of the $m = 0$ mode at the chromaticity at which its spectrum becomes double-peaked appears in the overall threshold current, since there are no higher order modes to limit the threshold current in this region. This is seen in the time domain results and in the frequency domain and justifies ignoring the $|m| > 0$ modes altogether.

The non-Gaussian beam distribution means that the frequency spectrum of the $m = 0$ head-tail mode is not simply single or double peaked but has ripples in the tails. These ripples interact with the impedance, adding some periodic structure to the threshold current curve as oscillations appear between the main peaks in the spectrum. This behavior is more dominant with shorter bunch lengths. This has been seen in frequency domain calculations applying Laclare's eigenvalue method to non-Gaussian distributions and in the analysis of time domain simulations of instabilities in the flat potential condition.

The fourth and final difference made by the flat potential is the nonradial bunch distribution and this cannot be treated using Laclare's eigenvalue method. The bunch in the flat potential has a Gaussian distribution in energy but goes as $e^{-a\tau^4}$ in time offset τ (where a is a constant). Accordingly, the synchrotron motion contains significant components at odd harmonics of the synchrotron frequency. By elimination, it must be concluded that it is this fourth feature that accounts for the remaining difference seen between the time domain simulations of the flat potential condition and the frequency domain calculations of similar bunch profiles. Slight differences in bunch profile, between flattened and semielliptical for example, do not have a sufficient impact to explain the difference seen in threshold current and the time domain and frequency domain results otherwise agree very well. Above a certain chromaticity, the frequency domain calculations that assume radial distributions appear to underestimate the threshold current by a constant factor of around 1.6 compared to the more accurate time domain simulations. Below this chromaticity, the factor approaches 1.6 from below as the chromaticity is increased. This factor quantifies the contribution of the nonradial distribution.

An intermediate bunch length was also investigated in order to gain a deeper insight into the role that the bunch length plays. With and without harmonic cavities, increasing the bunch length results in an inverse scaling along the horizontal axis of the curves of threshold current against chromaticity. There are differences beyond this scaling because the narrower spectra of the longer bunches cover fewer of the frequencies given by Eq. (2). These differences include the size of the peaks in the threshold current due to the oscillations seen between the main peaks in the bunch spectra with the flat potential condition.

The results in this paper suggest that the nominal chromaticity for the MAX IV 3 GeV ring of $+1$ may not be the ideal value in terms of beam stability against the resistive-wall impedance. A lower chromaticity may coincide with a large peak in the threshold current as well as providing the additional benefits in terms of the transverse dynamic aperture and beam lifetime. However, since the main goal of this paper was to illustrate the physical mechanism behind the stabilization by the harmonic cavities at MAX IV, only the resistive wall and, in one case, a single BBR have been included in the impedance models. It was seen that the effect of the BBR was to stabilize the beam below a certain chromaticity that is dependent on the bunch length and then to destabilize the beam above this chromaticity. The full ring impedance model of the bare machine contains 12 BBRs in the vertical plane [11] that are likely to have a large effect on the threshold currents. Using MBTRACK, which can treat both longitudinal and transverse wakefields simultaneously, the full MAX IV impedance model including the longitudinal resistive wall and geometric impedance could be included. The predicted microwave threshold for the MAX IV 3 GeV ring is 12 mA per bunch with harmonic cavities and 10 mA without [16] (corresponding to 2112 mA and 1760 mA total current respectively). This is significantly larger than the vast majority of threshold currents presented in this paper so the turbulent regime need not be considered. However, bunch lengthening due to longitudinal impedance could be an important factor. This could be checked

using RWMBI by simply adjusting the input bunch length accordingly. Finally, the threshold current presented here is calculated by equating the inverse growth rate of the transverse coupled-bunch instability to the radiation damping time. Adding a basic model of the radiation damping to the time domain simulations can lead to significantly higher threshold currents [26]. The growth rate was also assumed to be proportional to current when it is known that, as the current is increased, the proportionality is broken due to the change in the coherent betatron frequency and the interaction of the different head-tail modes.

ACKNOWLEDGMENTS

The computing time was on the SOLEIL cluster, for which, the authors would like to thank Alejandro Dias-Ortiz and Phillipe Martinez for their continuing support. The implementation of harmonic cavities in MBTRACK was the work of Marit Klein. The authors are grateful for financial support through the Swedish Research Council funded Cooperation in the field of synchrotron light research between SOLEIL and MAX IV. The research leading to these results has received funding from the European Commission under the FP7 Research Infrastructure project EuCARD-2, Grant Agreement No. 312453.

[1] P. F. Tavares, S. C. Leemann, M. Sjöström, and Å. Andersson, The MAXIV storage ring project, J. Synchrotron Radiat. **21**, 862 (2014).

[2] E. Al-Dmour, J. Ahlback, D. Einfeld, P. F. Tavares, and M. Grabski, Diffraction-limited storage-ring vacuum technology, J. Synchrotron Radiat. **21**, 878 (2014).

[3] K. L. F. Bane and M. Sands, The short range resistive wall wake fields, AIP Conf. Proc. **367**, 131 (1996).

[4] P. F. Tavares, Å. Andersson, A. Hansson, and J. Breunlin, Equilibrium bunch density distribution with passive harmonic cavities in a storage ring, Phys. Rev. ST Accel. Beams **17**, 064401 (2014).

[5] A. Hofmann and S. Myers, CERN Technical Report No. ISR-TH-RF/80-26, 1980.

[6] J. M. Byrd and M. Georgsson, Lifetime increase using passive harmonic cavities in synchrotron light sources, Phys. Rev. ST Accel. Beams **4**, 030701 (2001).

[7] M. Georgsson, Å. Andersson, and M. Eriksson, Landau cavities at MAX II, Nucl. Instrum. Methods **416**, 465 (1998).

[8] M. Svandrlik *et al.*, in *Proceedings of the 11th Workshop on RF Superconductivity, Lübeck, Germany, 2003* (DESY, Hamburg, 2003).

[9] M. Pedrozzi *et al.*, in *Proceedings of the 11th Workshop on RF Superconductivity, Lübeck, Germany, 2003* (DESY, Hamburg, 2003).

[10] W. Anders and P. Kuske, in *Proceedings of the 2003 Particle Accelerator Conference, Portland, OR* (IEEE, New York, 2003), p. 1186.

[11] G. Skripka, P. F. Tavares, M. Klein, and R. Nagaoka, in *Proceedings of the 5th International Particle Accelerator Conference, Dresden, Germany, 2014* (EPS-AG, Mulhouse, 2014).

[12] Y. H. Chin, Instability of a bunched beam with synchrotron-frequency spread, Part. Accel. **13**, 45 (1983).

[13] A. Burov, Nested head-tail Vlasov solver, Phys. Rev. ST Accel. Beams **17**, 021007 (2014).

[14] Y. H. Chin, Longitudinal stability limit for electron bunches in a double rf system, Nucl. Instrum. Methods Phys. Res. **215**, 501 (1983).

[15] R. A. Bosch, K. J. Kleman, and J. J. Bisognano, Robinson instabilities with a higher harmonic cavity, Phys. Rev. ST Accel. Beams **4**, 074401 (2001).

[16] G. Skripka, R. Nagaoka, M. Klein, F. Cullinan, and P. F. Tavares, Simultaneous computation of intrabunch and interbunch collective beam motions in storage rings, Nucl. Instrum. Methods **806**, 221 (2016).

[17] J. L. Laclare, CERN Accelerator School Report No. 87–03, p. 306, (CERN, Geneva, 1987).

[18] R. Nagaoka and K. L. F. Bane, Collective effects in a diffraction-limited storage ring, J. Synchrotron Radiat. **21**, 937 (2014).

[19] F. Cullinan, R. Nagaoka, G. Skripka, and P. F. Tavares, in *Proceedings of the 6th International Particle Accelerator Conference, Richmond, 2015* (IEEE, New York, 2015).

[20] P. Kernel, Ph.D. thesis, University Joseph Fourier, Grenoble, France, (2000).

[21] W. Rosenheinrich, EAH University of Applied Sciences Report, *Tables of some indefinite integrals of Bessel functions* (2003).

[22] F. J. Sacherer, in *Proceedings of the 9th International Conference on High-energy Accelerators, Stanford, CA* (AEC, Washington DC, 1975).

[23] P. Kernel, J.-L. Revol, R. Nagaoka, and G. Besnier, in *Proceedings of the 18th Particle Accelerator Conference, New York, 1999* (IEEE, New York, 1999).

[24] M. Klein and R. Nagaoka, in *Proceedings of the 4th International Particle Accelerator Conference, IPAC-2013, Shanghai, China, 2013* (JACoW, Shanghai, China, 2013).

[25] R. Nagaoka, rwmbi: A frequency domain solution of transverse coupled-bunch instability driven by resistive-wall and broad-band impedance (unpublished).

[26] A. Passarelli, H. Bartosik, O. Boine-Frankenheim, and G. Rumolo, in *2nd Topical Workshop on Instabilities, Impedance and Collective Effects, Abingdon, UK, 2016* (2016).